International Journal of Innovation and Applied Studies
ISSN 2028-9324 Vol. 48 No. 3 May. 2026, pp. 998-1006

http://www.ijias.issr-journals.org/

Soil quality decline along a forest-savanna gradient drives vegetation cover dynamics in the Comoé National Park (Côte d'Ivoire)

Konaté Alassane[1], Bongoua-Devisme Affi Jeanne[1], Dibi N'Da Hyppolite[2], and Akotto Odi Faustin[1]

[1]Laboratoire de Pédologie et Agriculture Durable, UFR Sciences de la Terre et des Ressources Minières, Université Félix Houphouët-Boigny, Abidjan, Côte d'Ivoire

[2]Centre Universitaire de Recherche et d'Application en Télédétection (CURAT), Université Félix Houphouët-Boigny, Abidjan, Côte d'Ivoire

ABSTRACT: Soil quality is a key determinant of vegetation cover dynamics in tropical protected areas, yet its quantitative relationship with vegetation degradation under anthropogenic pressure remains poorly documented at the profile scale in West African savannas. This study, carried out in Comoé National Park (CNP, north-eastern Côte d'Ivoire), tested the hypothesis that the forest-savanna vegetation gradient along an approximately 800 m transect of the corresponds to a measurable decline in soil quality driven by increasing anthropogenic pressure at the park periphery. Five pedological profiles were excavated in March 2023, morphologically described and analysed following ISRIC protocols, and classified using WRB 2022. Clay cation exchange capacity (clay-CEC) and available phosphorus (P) were used as primary soil quality indicators. Results revealed a systematic soil quality gradient from gallery forest to degraded tree savanna: clay-CEC in the argillic horizon decreased from 27.4 cmol (c) kg^{-1} (Ferric Lixisol, gallery forest) to 9.5 cmol (c) kg^{-1} (Ferric Acrisol, degraded savanna), while available P declined from 16.3 to 0.1–1.4 mg kg^{-1}. Three mid-slope profiles classified as Stagnic Ferric Acrisols showed temporary waterlogging from 10–11 cm depth and near-complete P immobilisation, directly constraining rooting depth and woody species regeneration. Two pedological anomalies were documented: MnO_2-mediated pH buffering (pH 7.0) and smectite neoformation (CEC = 148 $mmol^+$ kg^{-1}) under pseudo-gley conditions. These findings establish a quantitative edaphic basis for vegetation cover decline in the CNP periphery and support differentiated conservation management strategies.

KEYWORDS: Lixisol, Acrisol, soil-vegetation relationship, clay-CEC, Comoé National Park, Côte d'Ivoire.

1 INTRODUCTION

Soils of the West African Sudanian savannas play a fundamental role in natural ecosystem dynamics and the resilience of agricultural systems against climatic and anthropogenic disturbances [1]. Their capacity to support woody vegetation, store carbon, and regulate hydrological cycles depends on edaphic properties that vary strongly across landscapes according to topography, lithology, and land use history [2]. Yet the quantitative relationship between soil quality and vegetation cover dynamics at the profile scale remains poorly documented in West African protected ecosystems.

The Comoé National Park (CNP, north-eastern Côte d'Ivoire), the largest protected area in West Africa (11,500 km^2, UNESCO World Heritage Site), constitutes a privileged observatory for soil-vegetation interactions. Its ecosystems are subjected to increasing anthropogenic pressure at the periphery (clearing, shifting cultivation, transhumance) documented by multiple studies on vegetation cover degradation [3], [4], [5] and land use change [6], [7], [8]. In contrast, systematic pedological investigations remain scarce: the work of Roose [9] and BUNASOLS [10] established the broad regional cartographic units, but without the analytical resolution necessary to link soil properties to vegetation at the transect scale.

The WRB 2022 classification system (World Reference Base for Soil Resources, IUSS Working Group WRB, 2022) [11], based on strict analytical criteria, particularly clay cation exchange capacity (clay-CEC) as the discriminating criterion between Lixisols (≥.24 cmol (c) /kg in the argillic horizon) and Acrisols (< 24 cmol (c) /kg), provides a rigorous and internationally comparable framework for characterising the pedological diversity of this environment. We hypothesise that the vegetation gradient observed along transect L1 corresponds to a measurable pedogenetic gradient in which clay-CEC and phosphorus availability are the most discriminating indicators of soil quality decline.

Corresponding Author: Akotto Odi Faustin

2 MATERIAL AND METHODS

2.1 STUDY AREA

The study site is the Comoé National Park (CNP), located between 8°30' and 9°40' N and 3°10' and 4°20' W (Fig. 1), covering approximately 1,149,150 ha. The climate is tropical subhumid (Köppen: Aw), with mean annual precipitation of 900–1,100 mm. The dominant vegetation is Sudanian wooded savanna with *Isoberlinia doka, Daniellia oliveri,* and *Vitellaria paradoxa,* with gallery forests along waterways (*Khaya senegalensis, Ceiba pentandra*). The parent material is Precambrian granite-gneiss basement. The five profiled soils span a toposequential sequence from gallery forest (L1-P1, 201 m) to degraded tree savanna (L1-P6, 190 m), covering approximately 800 m.

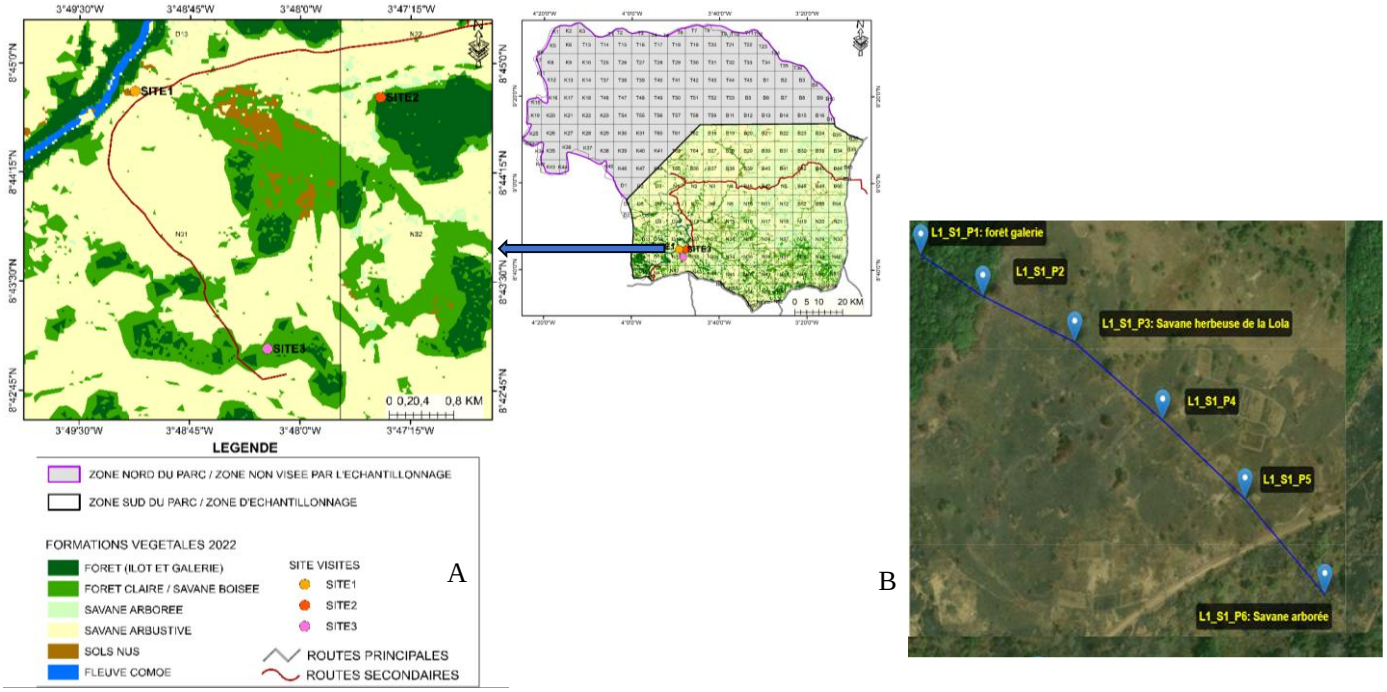

Fig. 1. Location of the study area - A. Study site; B. Toposequential sequence of transect L1, Comoé National Park, Côte d'Ivoire

2.2 FIELD SAMPLING AND PROFILE DESCRIPTION

Profiles were excavated in March 2023 (end of dry season). Pedological pits (1.5 m x 1.0 m, depth 0.7-1.2 m) were described following the FAO Guide for the IUSS WRB Working Group (2022). GPS coordinates (UTM, Zone 30N, WGS84) and altitudes were recorded by differential GNSS (±2 m precision). Munsell colours were determined on moist and dry soil using the Munsell 2009 chart. Coarse elements were estimated visually and verified by sieving (2 mm sieve).

2.3 LABORATORY ANALYSES

Soil samples (500 g per horizon) were air-dried, crushed, and sieved at 2 mm. All analytical methods follow ISRIC protocols [12]: particle-size distribution by the Robinson pipette method (5 fractions) after H_2O_2 treatment and sodium pyrophosphate dispersion; organic carbon by Walkley-Black method; total nitrogen by Kjeldahl; pH (H_2O and KCl) at 1: 2.5 ratio; CEC and exchangeable bases by ammonium acetate extraction at pH 7.0 (Metson method); available phosphorus by Bray II method; coarse elements by sieving and weighing at 105°C. For profile L1-P4, MnO_2 nodules were confirmed by H_2O_2/HCl decolourisation test.

2.4 SOIL CLASSIFICATION

The primary classification is WRB 2022. Parallel systems used are Soil Taxonomy (USDA 1999), FAO (1974), and CPCS. Clay-CEC (= CEC / (% clay / 100)) is the key criterion discriminating Lixisols from Acrisols. The WRB 2022 procedure was applied sequentially: (i) ochric horizon verification; (ii) argillic horizon (clay ratio B/A ≥ 1.2); (iii) Lixisol/Acrisol discrimination; (iv) first-level qualifiers (*Ferric, Stagnic, Endopetric*); (v) second-level qualifiers (*Dystric, Skeletic*).

3 RESULTS

3.1 OVERVIEW OF THE L1 TOPOSEQUENCE

The five profiles span 11 m of altitude (201-190 m) and represent a complete ecological gradient from gallery forest to degraded tree savanna. Table 1 summarises the WRB 2022 classification, key clay-CEC values and drainage conditions.

Table 1. WRB 2022 classification, clay-CEC of the argillic horizon and Stagnic depth along transect L1, Comoé National Park

Profile	Site / Vegetation	Alt. (m)	Clay-CEC argic (cmol(c)/kg)	Stagnic depth	WRB 2022 Classification
L1-P1	Gallery forest	201	27.4	None	Ferric Lixisol (Dystric, Skeletic)
L1-P3	Grass savanna	201	21.2	10 cm	Stagnic Ferric Acrisol (Dystric)
L1-P4	Degraded wooded savanna	199	16.8	11 cm	Stagnic Ferric Acrisol (Dystric, Endopetric)
L1-P5	Shrub savanna	196	10.7-21.2	11 cm	Stagnic Ferric Acrisol (Dystric, Endopetric)
L1-P6	Degraded tree savanna	190	9.5	None	Ferric Acrisol (Dystric, Endopetric)

3.2 FERRIC LIXISOL (DYSTRIC, SKELETIC) L1-P1 - GALLERY FOREST

Situated at 201 m in gallery forest, L1-P1 (Fig. 2) is the only Lixisol on the transect. Clay-CEC in the argillic horizon B1.2 (94-110 cm) reaches 27.4 cmol (c).kg^{-1}, exceeding the WRB 2022 threshold, reflecting 2: 1 clay minerals (illite, interstratified) inherited from gentle weathering under dense forest. Available phosphorus is highest at the surface (16.3 mg.kg^{-1}), base saturation exceeds 79% throughout, and pH ranges 6.2-6.5. The 60 % coarse elements in A0 (argillaceous aggregates) justifies the *Skeletic* suffix; ferruginous concretions ≥ 15% in B1.1 justify the *Ferric* prefix.

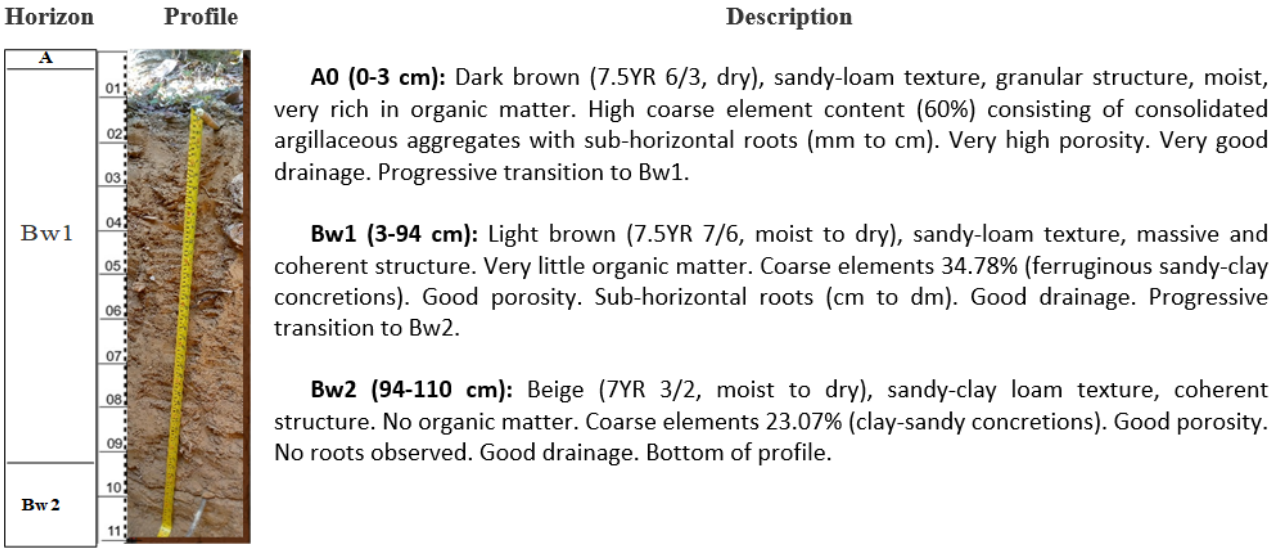

Fig. 2. Morphological description of profile L1-P1 Ferric Lixisol (Dystric, Skeletic) - Gallery Forest, Bouna, Comoé National Park. UTM coordinates: N 967163 / W 409911, altitude 201 m, March 25, 2023

3.3 STAGNIC FERRIC ACRISOL (DYSTRIC, ENDOPETRIC) - GRASS SAVANNA

Both profiles L1-P3 and L1-P4 (Fig. 3 and Fig. 4) show redoximorphic features from 10-11 cm, indicating seasonal perched water tables above the compact argillic horizon. In L1-P3, the diagnostic Btg horizon (10-26 cm, 49% clay) has clay-CEC = 21.2 cmol (c).kg^{-1} < 24, confirming Acrisol classification. Available P drops from 3.6 mg.kg^{-1} (A1) to 0.1-1.3 mg.kg^{-1} (deep Bcg). In L1-P4, clay-CEC falls to 16.8 cmol (c).kg^{-1} in the argillic Btg (11-23 cm), the second lowest on the transect. A remarkable pH anomaly in Bcg2 (61-100 cm): pH 7.0 and positive ΔpH (+1.1), attributed to MnO_2 reduction (see Section 4.3). Ferruginous induration at 90 cm classifies L1-P4 as *Endopetric*.

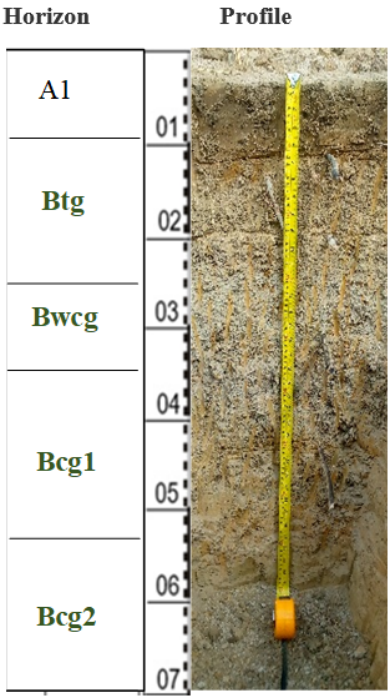

Description

A1 (0-10 cm): Dark greyish brown (2.5Y 3/2, moist), loamy clay texture (34 % clay), well-developed granular structure, OM = 1.40%, numerous roots, good drainage. Sharp transition to Btg,

Btg (10-26 cm): Pale beige (2.5Y 6/2, moist to dry), clayey texture (49 % clay). Argillic horizon (t) with hydromorphic features from 10 cm (g); 22.72% clay-ferrous concretions; clay-CEC = 21.2 cmol(c) kg^{-1} (Acrisol). Low porosity. Few centimetric roots. Poor drainage (temporary waterlogging). Irregular transition to Bwcg,

Bwcg (26-36 cm): Mottled brown (5Y 4/2, dry), sandy-loam texture (14% clay) marked textural break from Btg (49 to 14 %). Particulate structure (no cohesion). No organic matter. 20 % ferrous concretions with oxidation and hydromorphic mottles. Low porosity. Rare roots. Poor drainage. Progressive transition to Bcg1,

Bcg1 (36-53 cm): Dull brownish red (10YR 3/2, dry), sandy-clay loam texture (31% clay). Massive compact structure. No organic matter. 12 % ferrous concretions (incipient induration). Very low porosity. Rare roots. Very poor drainage. Progressive transition to Bcg2,

Bcg2 (53-70 cm): Dull brownish red with intense rust mottles (10YR 5/2, dry), clayey texture (43 % clay). Massive structure. No organic matter. 15 % iron and clay concretions. Very low porosity. Rare roots. Very poor drainage. Intense rust mottles indicate iron oxidation during drying phases after waterlogging. Bottom of profile.

Fig. 3. Morphological profile of L1-P3 Stagnic Ferric Acrisol (Dystric, Endopetric), grass savanna, Bouna, Comoé National Park. UTM: N 967096 / W 410054, altitude 201 m, March 24, 2023

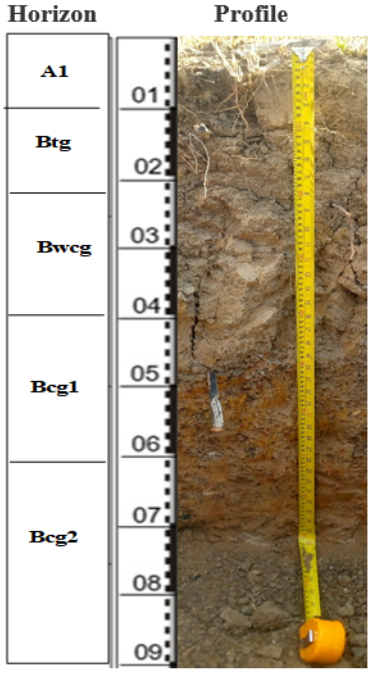

Description

A1 (0-11 cm): Dark brown (10YR 3/3, moist), loamy clay texture (20 % clay), well-developed granular structure, OM = 1.47%, signs of anthropogenic compaction. Sharp transition to Btg.

Btg (11-23 cm): Yellowish brown (7.5YR 5/6, moist), clayey texture (38 % clay)-abrupt clay increase from A1 (20 to 38 %), ratio Btg/A1 = 1.90, well above the WRB argillic threshold of 1.2. Argillic horizon (t) with redoximorphic features (g). Clay-CEC = 16.8 cmol(c) kg^{-1} < 24 (Acrisol). 18 % clay concretions with hydromorphic mottles. Low porosity. Few centimetric roots. Poor drainage. Irregular transition to Bwcg.

Bwcg (23-40 cm): Mottled yellowish brown (10YR 5/4, moist), clayey texture (39 % clay). *In-situ* alteration (w) + concretions (c) + redox mottles (g). 20 % ferruginous concretions with intense oxidation mottles. Particulate structure. No organic matter. Rare roots. Poor drainage. Progressive transition to Bcg1.

Bcg1 (40-61 cm): Brown (7.5YR 4/6, moist), sandy-clay texture (22% clay). Black MnO_2 mottles; clay-CEC = 20.9 < 24; pronounced waterlogging. Massive compact structure. No organic matter. 25% coarse elements. Very low porosity. Rare roots. Very poor drainage. Progressive transition to Bcg2,

Bcg2 (61-90 cm): Olive brown (5Y 5/3, moist), clayey texture (36 % clay). pH = 7.0 anomaly; abundant MnO_2 nodules; induration at 90 cm (Endopetric); refusal at 100 cm. Positive ΔpH (+1.1) indicates net positive variable charge. Massive structure. No organic matter. 30% coarse elements. Very low porosity. No roots. Very poor drainage. Bottom of profile.

Fig. 4. Morphological profile of L1-P4 Stagnic Ferric Acrisol (Dystric, Endopetric), degraded wooded savanna, Nassian periphery, Comoé National Park. UTM: N 967036 / W 410136, altitude 199 m, March 24, 2023

3.4 STAGNIC FERRIC ACRISOL (DYSTRIC, ENDOPETRIC) - L1-P5 - SHRUB SAVANNA

Profile L1-P5 (196 m, Nassian) presents a high CEC (14.8 cmol (c).kg^{-1}) in the Btg horizon (11-50 cm), interpreted as a smectite neoformation signature under pseudo-gley conditions (colour 5Y 7/3). Clay-CEC drops to 10.7-21.2 cmol (c). kg^{-1} in the Bpfg horizon (50-91 cm), confirming Acrisol classification. Available P is near-zero throughout depth (0.1–0.3 mg.kg^{-1}). Ferruginous induration begins at 50 cm (Fig.5).

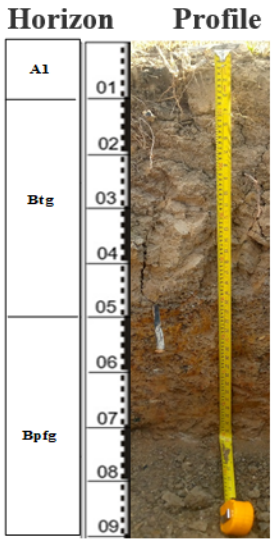

Description

A1 (0-11 cm): Dark brown (7.5YR 6/3, moist), sandy-clay loam texture (26 % clay), granular structure, OM = 1.38 %, 34.78 % argillaceous aggregates, abundant sub-horizontal roots (mm to cm). Very good porosity. Very good drainage. Progressive transition to Btg.

Btg (11-50 cm): Beige pseudo-gley (5Y 7/3, dry), characteristic colour of intense seasonal waterlogging. Clayey texture (46-52 % clay according to sampling depth). Clay accumulation ratio 1.77-2.00, well above the WRB threshold of 1.2. Argillic horizon (t) + hydromorphic features (g). 8.33 % oxidising argillaceous concretions. CEC = 148 $mmol^{+}\ kg^{-1}$, exceptional value suggesting smectite neoformation under pseudo-gley conditions. Massive structure. Low porosity. Rare centimetric to decimetric roots. Poor drainage. Irregular transition to Bpfg.

Bpfg (50-91 cm): Mottled red (10YR 5/2, dry), clayey texture (45-49 % clay). Incipient Petroferric horizon (pf) with ferruginous induration from 50 cm (Endopetric). Quartz vein from Precambrian basement (granite) visible below 50 cm. Very poor drainage with intense oxidation traces. 8.82% coarse elements. No roots. Very low porosity. Bottom of profile with generalised induration beyond 90 cm..

Fig. 5. Morphological profile of L1-P5 Stagnic Ferric Acrisol (Dystric, Endopetric), shrub savanna, Kakpin-Nassian, Comoé National Park. UTM: N 966975 / W 410213, altitude 196 m, March 24, 2023

3.5 FERRIC ACRISOL (DYSTRIC, ENDOPETRIC) - L1-P6 - DEGRADED TREE SAVANNA

Profile L1-P6 (190 m) is the most ferrallitised, with absolute minimum clay-CEC of 9.5 cmol (c).kg^{-1} in the argillic Bt1 (20-59 cm). Unlike L1-P3-P5, L1-P6 shows no Stagnic features (vivid colours exclusively 5YR/7.5YR), indicating effective drainage, likely facilitated by the macroporosity of pysoplentique ferruginous concretions. Unaltered quartz and feldspar crystals in Bt2 (59-74 cm) signal a shallow lithological contact with Precambrian granite. Available P in A1 (5.5 $mg.kg^{-1}$) is slightly higher than in L1-P3/P4 (Fig. 6), attributed to transitional P release from weathering feldspars.

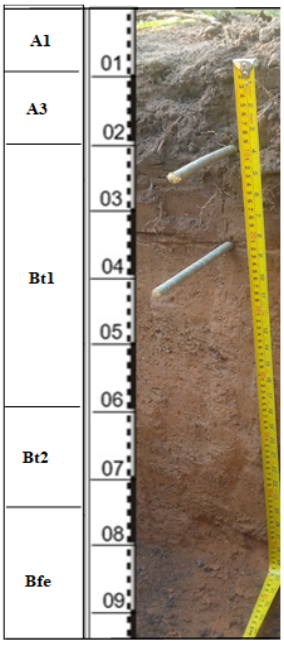

Description

A1 (0-9 cm): Dark brown (7.5YR 3/4, moist), sandy-loam texture (16% clay), granular coherent structure, OM = 1.21 %, 44% argillaceous aggregates (intense biological pedoturbation by termites and burrowing fauna). Good porosity. Numerous roots (mm to cm). Good drainage. Irregular transition to A3.

A3 (9-20 cm): Dark to pale brown (7.5YR 6/6, moist), clayey texture (46 % clay), partially humiferous (OM = 1.21 %), incipient oxidising concretions (36.36 %). Coherent to subangular blocky structure. C/N = 7.8: highly mineralised organic matter. Medium drainage. Irregular transition to Bt1.

Bt1 (20-59 cm): Brun rougeâtre (5YR 6/8, frais à sec). Argile (40 %). Horizon argilique principal : ratio Bt1/A1 = 2,50. Couleur 5YR témoigne de sesquioxydes de Fe libres (goethite/hématite). EG = 35,71 % de concrétions pysoplentiques (ferrugination avancée). Structure massive et cohérente. pH 5,3; CEC = 3,8 cmol(c)/kg; CEC argile = 9,5 cmol(c)/kg. Transition progressive vers Bt2,

Bt2 (59-74 cm): Reddish brown (5YR 5/8, dry), clayey texture (42 % clay). Lower argillic horizon. Unaltered quartz and feldspar crystals visible (23.68 % coarse elements) shallow lithological contact with Precambrian granite (granite or gneiss). Massive structure. Poor drainage. Few rare millimetric roots. Progressive transition to Bfe.

Bfe (74-94 cm): Brown-red with ochre red mottles (5YR 5/8 mottled, dry), clayey texture (41 % clay). Dense pysoplentique clay concretions (22.85 %) + ferruginous induration at 85 cm (Endopetric). Subangular fragmentary structure. No roots. Very low porosity. pH rises to 6.1 (Fe/Al oxide buffering). Active lateritisation beyond 85 cm. Bottom of profile.

Fig. 6. Morphological profile of L1-P6 - Ferric Acrisol (Dystric, Endopetric), degraded tree savanna, Nassian, Comoé National Park. UTM: N 966990 / W 410287, altitude 190 m, March 25, 2023

3.6 ANALYTICAL SUMMARY

The five profiles of transect L1 form a coherent pedogenetic sequence whose morphological expression (Figures 2-6) is fully consistent with the analytical data summarised in Tables 2 and 3. Three convergent gradients structure this sequence.

A systematic decline in clay-CEC. The diagnostic argillic horizon shows a monotonic decrease in clay-CEC from 27.4 cmol (c) kg^{-1} in the gallery-forest Lixisol to 9.5 cmol (c) kg^{-1} in the degraded tree-savanna Acrisol, crossing the WRB 2022 discrimination threshold of 24 cmol (c) kg^{-1} between L1-P1 and L1-P3 (Table 1). This transition from 2: 1 clay minerals under gallery forest to kaolinite-dominated assemblages under open savanna is visually expressed by the progressive change in horizon colouration (from the beige-brown tones of L1-P1 to the vivid reddish-brown 5YR hues of L1-P6 Bt1) and is confirmed by the systematically lower CEC values throughout the argillic horizons of L1-P3 through L1-P6 (Table 2).

A progressive onset and intensification of waterlogging. The absence of redoximorphic features in L1-P1 and L1-P6 contrasts sharply with the Stagnic features documented from 10-11 cm in L1-P3, L1-P4, and L1-P5. The distinctive pale beige pseudo-gley colour (5Y 7/3) of the Btg horizon in L1-P5 is the most visually striking expression of this waterlogging, consistent with the exceptional CEC of 148 $mmol^{+}$ kg^{-1} recorded in Table 2 and interpreted as smectite neoformation under alternating redox conditions. In L1-P4, the blackish MnO_2 nodules visible in Bcg2 directly correspond to the pH 7.0 anomaly and positive ΔpH (+1.1) reported in Table 2.

A near-complete phosphorus collapse. Available P in the surface horizon drops from 16.3 mg kg^{-1} under gallery forest to 1.4-3.6 mg kg^{-1} under savanna (L1-P3, L1-P4, L1-P5), reflecting the progressive loss of organic litter input visible in the thinning and darkening of surface A horizons across. The slightly elevated P in L1-P6 A1 (5.5 mg $kg^{-1,}$ Table 1) is a transitional anomaly attributable to incipient feldspar weathering, as confirmed by the unaltered quartz and feldspar crystals visible in the Bt2 horizon of Figure 6 (a morphological feature unique to this profile on the transect).

Taken together, the morphological profiles (Figures 2-6) and analytical tables (Tables 2-3) establish that the forest-savanna vegetation gradient along transect L1 is underpinned by a measurable, multi-indicator soil quality decline, operating simultaneously on clay mineralogy, drainage regime, and phosphorus availability: three edaphic functions directly controlling woody species establishment and vegetation cover dynamics in the Comoé National Park periphery

Table 2. Summary of WRB 2022 classification and key analytical parameters for the five profiles of transect L1, Comoé National Park. CECclay = clay cation exchange capacity in the diagnostic argillic horizon (*); V = base saturation (pH 7 ammonium acetate); P_{avail} = available phosphorus (Bray II) in the surface horizon

Profile	Vegetation	Clay ratio B/A	CECclay* (cmol/kg)	Stagnic (depth cm)	P avail. mg/kg	WRB 2022
L1-P1	Gallery forest	2.50	27.4	None	16.3	Ferric Lixisol (Dystric, Skeletic)
L1-P3	Wooded savanna	1.44	21.2	Yes (10)	3.6	Stagnic Ferric Acrisol (Dystric)
L1-P4	Degraded savanna	1.90	16.8≠	Yes (11)	2.1	Stagnic Ferric Acrisol (Dystric, Endopetric)
L1-P5	Degraded savanna	1.77-2.00	10.7≠	Yes (11)	1.4	Stagnic Ferric Acrisol (Dystric, Endopetric)
L1-P6	Tree savanna	2.50	9.5	None	5.5§	Ferric Acrisol (Dystric, Endopetric)

≠pH anomaly (7.0) in Bcg2 attributed to MnO_2 nodule dissolution. ≠Btg-1 CEC = 148 $mmol^{+}$ kg^{-1} (smectite neoformation); minimum CECclay in Bpfg. § Elevated P from incipient feldspar weathering.

Table 3. Detailed analytical data (chemistry and clay-CEC) for all profile horizons. OC = organic carbon; CEC = cation exchange capacity; V = base saturation; ΔpH = pH (KCl) – pH (H_2O)

Profile	Horizon	Depth (cm)	pHH_2O	OC (%)	Clay (%)	CEC cmol/kg	V (%)	CECclay cmol/kg	ΔpH
L1-P1	A0	0-3	6.2	0.84	6	4.7	79	78.3	−0.9
	B1.1	3-94	6.4	0.46	15	5.6	80	37.3	−0.9
	B1.2	94-110	6.5	0.34	27	7.4	80	27.4*	−0.9
L1-P3	A1	0-10	6.1	0.81	34	7.7	76	22.6	−1.1
	Btg	10-26	6.8	0.43	49	10.4	77	21.2*	−0.9
	Bwcg	26-36	6.3	0.35	14	5.6	76	40.0⊀	−0.9
	Bcg1	36-53	6.5	0.38	31	6.5	78	20.6	−0.9
	Bcg2	53-70	6.6	0.35	43	11.3	77	25.1	−0.9
L1-P4	A1	0-11	6.0	0.85	20	6.8	82	34.0	−0.9
	Btg	11-23	6.2	0.58	38	6.4	80	16.8*	−0.9
	Bwcg	23-40	6.3	0.45	39	7.8	80	20.0	−0.9
	Bcg1	40-61	6.5	0.38	22	4.6	83	20.9	−0.9
	Bcg2	61-100	7.0⊀	0.32	36	11.3	89	31.4⊀	+1.1‡
L1-P5	A0	0-11	6.6	0.80	26	8.1	83	31.2	−1.1
	Btg-1	11-50s	6.6	0.55	46	14.8§	83	32.2	−1.1
	Btg-2	11-50i	6.7	0.54	52	-	-	-	−1.1
	Bpfg-1	50-91s	6.4	0.43	49	10.4	82	21.2*	−1.1
	Bpfg-2	50-91i	5.6	0.52	45	4.8	85	10.7*	−1.1
L1-P6	A1	0-9	6.6	0.70	16	4.5	88	28.1	−1.1
	A3	9-20	5.9	0.70	46	6.0	83	13.0	−1.1
	Bt1	20-59	5.3	0.45	40	3.8	84	9.5*	−1.1
	Bt2	59-74	5.6	0.44	42	4.9	83	11.7	−1.1
	Bfe	74-94	6.1	0.44	41	5.6	84	13.7	−1.1

**Diagnostic argillic horizon. ⊀Artefact: CECclay inflated by very low clay content (14 %); not used for classification. ⊀Bcg2 pH anomaly and positive ΔpH attributed to MnO_2 dissolution. CEC = 148 mmol$^+$ kg^{-1}; interpreted as smectite neoformation. s = upper sub-sample; i = lower sub-sample.*

4 DISCUSSION

4.1 CLAY-CEC AS DISCRIMINATING CRITERION BETWEEN LIXISOLS AND ACRISOLS

The 24 cmol (c) kg^{-1} threshold clearly separates L1-P1 (Ferric Lixisol, clay-CEC = 27.4) from profiles L1-P3 and L1-P4 (Acrisols, 16.8-21.2 cmol (c) /kg). This difference reflects distinct clay mineralogy: gallery forest Lixisols retain a kaolinitic-illitic fraction with high adsorptive capacity under gentle weathering and favourable drainage, whereas wooded-savanna Acrisols subject to more pronounced ferrallitisation and alternating drought–saturation cycles show declining clay-CEC through advanced kaolinisation and progressive replacement by low-charge iron oxides [13 [, [14]. L1-P4, at the CNP periphery (Nassian), has the lowest clay-CEC among the Stagnic Acrisols (16.8 cmol (c).kg^{-1}), consistent with more intense ferrallitisation and more persistent hydromorphic conditions. L1-P6, without Stagnic features but showing the most oxidising permanent conditions (colours 5YR/7.5YR throughout), reaches the absolute minimum of 9.5 cmol (c).kg$^{-1,}$ characteristic of kaolinite + Fe^{3+} oxides assemblage with minimal charge.

4.2 PROGRESSION OF STAGNIC FEATURES AND THEIR ECOLOGICAL SIGNIFICANCE

Profile L1-P1 is free of redoximorphic features, benefiting from lateral drainage under gallery forest. In contrast, L1-P3 and L1-P4 show Stagnic features from 10-11 cm, reflecting seasonal waterlogging in the wet season above the compact argillic horizon. This process, well-documented in Sudanian Acrisols [15], is amplified in L1-P4 by ferruginous induration at 90 cm blocking vertical percolation. The resulting shallow rooting constraint directly inhibits the establishment of deep-rooted woody species and contributes to the documented regression of tree cover at the CNP periphery.

4.3 MNO2-MEDIATED PH ANOMALY IN L1-P4 BCG2

The pH 7.0 and positive ΔpH (+1.1) in Bcg2 of L1-P4 are exceptional for a dystric Acrisol (typical pH < 6.5 at depth). Two non-exclusive mechanisms are proposed: (i) MnO_2 reduction under prolonged reducing conditions ($MnO_2 + 4H^+ + 2e^- \rightarrow Mn^{2+} + 2H_2O$), consuming protons and raising local pH; (ii) release of Ca^{2+} and Mg^{2+} during MnO_2 nodule dissolution, reaching the highest base saturation of the profile (V = 89.4%

in Bcg2). This manganese-mediated neutralisation is documented in ferruginous soils with manganiferous nodules in West Africa [16], [17]. Induration at 90 cm concentrates reducing reactions in this zone. The positive ΔpH (net positive variable charge) further confirms dominance of sesquioxides buffering at neutral-to-basic pH.

4.4 Phosphorus Availability As The Limiting Factor For Woody Vegetation

The P gradient (16.3 $mg.kg^{-1}$ in L1-P1 A0 to 0.1-1.3 $mg.kg^{-1}$ in deep Bcg of L1-P3/P4) constitutes the most direct edaphic constraint on vegetation recovery. In gallery forest, dense litter ensures continuous biological P recycling, moderate ferrallitisation allows organic matter to complex phosphate, and slightly acidic pH (6.2) limits P precipitation [18]. In savanna Acrisols, near-complete P immobilisation by Fe-Al sesquioxides at low organic matter content [19] prevents the mycorrhizal symbiosis and root growth required for woody pioneer species to establish on degraded surfaces. The slightly elevated P in L1-P6 A1 (5.5 $mg.kg^{-1}$) from weathering feldspars is a transient reservoir that will decline as weathering advances.

4.5 Smectite Neoformation Anomaly In L1-P5

The CEC of 148 $mmol^{+}\ kg^{-1}$ in the Btg-1 of L1-P5 is far above the kaolinite range (3-15 cmol (c).kg^{-1}) and constitutes a diagnostic signature of 2: 1 phyllosilicate neoformation. Seasonal waterlogging (colour 5Y 7/3) creates favourable hydrolysis conditions for crystallisation of montmorillonite or beidellite from dissolution of iron oxides and silica mobilisation [20], [21]. The 67% collapse of CEC from Btg to Bpfg-2, concomitant with colour change from 5Y to 10YR indicating return to oxidising conditions, confirms that smectites are confined to the pseudo-gley zone and replaced by kaolinite and Fe^{3+} oxides in depth [13]. This neogenesis produces a temporary local improvement of cation retention capacity in the waterlogged zone, but P immobilisation remains near-complete (0.1-0.3 $mg.kg^{-1}$).

4.6 Pedogenetic Gradient And Conservation Management

The decreasing clay-CEC gradient (78.3 to 9.5 cmol (c).kg^{-1} from L1-P1 to L1-P6), correlated with P decline (16.3 to 0.1-1.4 $mg.kg^{-1}$) and the progression of Stagnic and Endopetric features, reflects a systematic increase in ferrallitisation and edaphic impoverishment from the protected gallery forest toward the anthropogenic pressure zone at the CNP periphery [22], [23]. These results support differentiated conservation measures: strict protection of gallery forests (maintaining P stocks and biological soil structure as refugia for woody species regeneration), and rehabilitation of degraded Acrisols through adapted agroforestry (leguminous shrubs for N input and P solubilisation, wildfire management). The profiles at the CNP periphery (L1-P4, L1-P6) represent irreversible stages of soil degradation under current management [24]; restoration will require active intervention to re-introduce organic matter and break the impermeable ferruginous layers.

5 Conclusion

The pedological analysis of five profiles along transect L1 of the Comoé National Park, Bouna (Côte d'Ivoire) establishes a quantitative edaphic basis for vegetation cover decline along the forest-savanna gradient under anthropogenic pressure. The single gallery-forest Ferric Lixisol contrasts sharply with the three Stagnic Ferric Acrisols presenting early temporary waterlogging (10-11 cm), severe P immobilisation, and abundant ferruginous concretions. L1-P4 documents an exceptional MnO_2-mediated pH buffering; L1-P5 shows a smectite neoformation signature is the most ferrallitised profile, with the absolute minimum clay-CEC of 9.5 cmol (c) /kg, shallow lithological contact signalled by unaltered feldspars, and pysoplentique concretions evidencing advanced lateritisation. Clay-CEC of the argillic horizon is confirmed as a reliable and operationally relevant criterion for discriminating soil quality along this forest–savanna gradient in the Sudanian pedoclimatic context of West Africa. The correlated gradient of clay-CEC and available P provides a robust analytical foundation for soil–vegetation modelling and for prioritising differentiated habitat management at the CNP: strict protection of gallery forests and active rehabilitation of peripheral degraded Acrisols.

Acknowledgment

The authors thank the Direction des Parcs Nationaux de Côte d'Ivoire for granting field access authorisations, and the field teams for their logistical support. This work is part of a doctoral thesis funded by the Office Ivoirien des Parcs et Réserves (OIPR).

References

[1] Koueita, M., Konaté, K., Diomandé, M., Brou, A. N., 2018. La problématique de gestion du Parc National de la Comoé (PNC) en Côte d'Ivoire, entre la survie des populations riveraines et la conservation de la biodiversité. European Scientific Journal, 14 (35), 391–411. https://doi.org/10.19044/esj.2018.v14n35p391.

[2] V. Gond, «Contribution des données NOAA-AVHRR à la caractérisation des savanes africaines,» Ph.D. dissertation, Université Toulouse le Mirail, Toulouse, France, 1999. [Online]. Available: https://tel.archives-ouvertes.fr/tel-01239710.

[3] A. E. N'Guessan, N'J. Kassi, N. O. Yao, H. K. B. Amani, G. Z. R. Gouli, C. Piponiot, C. Z. Irie Bi, and B. Hérault, «Drivers of biomass recovery in a secondary forested landscape of West Africa,» *Forest Ecology and Management,* vol. 433, pp. 325–331, 2019. https://doi.org/10.1016/j.foreco.2018.11.021

[4] K. H. Koné, K. E. Konan, and Z. Koli Bi, «Caractérisation de la végétation du parc national de la Comoé (nord-est de la Côte d'Ivoire),» *Revue de Géographie Tropicale et d'Environnement,* no. 1, pp. 18–31, 2021.

[5] A. Konate, N. H. Dibi, and A. J. Bongoua-Devisme, «Analyse par télédétection de la dynamique des formations végétales 2002–2022 dans le Sud du Parc national de la Comoé (Nord-Est de la Côte d'Ivoire),» *European Scientific Journal, ESJ,* vol. 22, no. 3, p. 124, 2026. https://doi.org/10.19044/esj.2026.v22n3p124.

[6] Y. S. S. Barima, Dynamique, fragmentation et diversité végétale des paysages en milieux de transition forêt-savane dans le département de Tanda (Côte d'Ivoire). Doctoral thesis, Université libre de Bruxelles, Belgium, 2009.

[7] P. A. Silue, D. Soro, K. E. Kouassi, and D. Soro, «Dynamique d'occupation du sol et diversité floristique de la Forêt Classée de la Palé (Côte d'Ivoire),» *European Scientific Journal, ESJ,* vol. 17, no. 43, p. 1, 2021. https://doi.org/10.19044/esj.2021.v17n43p1.

[8] T. D. Soro, O. Blé Louan, J.-J. Koua Tanoh, A. Adjiri Oi, K. E. Ahoussi, G. Soro, M.-S. Oga Yei, and Soro Nagnin, «Suivi de la dynamique de l'occupation et de l'utilisation du sol dans le bassin versant du Haut Bandama à Tortiya (Nord de la Côte d'Ivoire) et son impact sur les écoulements,» *Environmental and Water Sciences, Public Health & Territorial Intelligence,* vol. 6, no. 1, pp. 754–760, 2022.

[9] E. Roose, Dynamique actuelle de sols ferrallitiques et ferrugineux tropicaux d'Afrique Occidentale: étude expérimentale des transferts hydrologiques et biologiques de matières sous végétations naturelles ou cultivées, Travaux et Documents de l'ORSTOM, no. 130. Paris: ORSTOM, 1981, 569 p. ISBN 2-7099-0594-9.

[10] BUNASOLS, Etude de reconnaissance des sols, région de Bouna. Burkina Faso, 1989.

[11] IUSS Working Group WRB (2022). World Reference Base for Soil Resources. International Soil Classification System for Naming Soils and Creating Legends for Soil Maps (4th ed.). International Union of Soil Sciences (IUSS).

[12] https://www.isric.org/sites/default/files/WRB_fourth_edition_2022-12-18.pdf

[13] L. P. van Reeuwijk, Procedures for Soil Analysis, 6th ed. Wageningen: ISRIC/FAO, 2002.

[14] B. Diop, I. Gbaguidi, P. Lo, A. Cisse, S. Sène and M. Ba, «Grain Size Influence on the Compaction Aptitude and the Bearing Strength of the Gravel Lateritic Soils,» *Geomaterials,* vol. 8, no. 4, pp. 63–76, 2018. doi: 10.4236/gm.2018.84005.

[15] T. Shibusawa, K. Tamura and M. Asano, «Anthropogenic Pedofeature in Andosols in Santome Shinden, One of the Representative Sites of the Satoyama Environment in Japan,» *Open Journal of Soil Science,* vol. 12, no. 12, pp. 586–604, 2022. https://doi.org/10.4236/ojss.2022.1212025.

[16] Z. Pang, Y. Zhang, S. Han, E. Wang and X. Chen, «Effects of Root Architecture on Uprooting Properties between Deciduous and Evergreen Species with Different Growth Habits,» *Forests,* vol. 15, p. 585, 2024. 585. https://doi.org/10.3390/f15040585.

[17] S. K. Obeng, M. Kulhánek, J. Balík, J. Černý and O. Sedlář, «Manganese: From Soil to Human Health-A Comprehensive Overview of Its Biological and Environmental Significance,» *Nutrients,* vol. 16, p. 3455, 2024. https://doi.org/10.3390/nu16203455.

[18] I. Sanchary and T. Akter, «Single and Sequential Extraction of Copper by Different Extractants from Different Peat Soil Samples of Bangladesh,» *Open Journal of Soil Science,* vol. 11, no. 12, pp. 611–627, 2021. doi: 10.4236/ojss.2021.1112030.

[19] G. Dowuona, P. Atwere, W. Dubbin, P. Nude, B. Mutala, E. Nartey and R. Heck, «Characteristics of Termite Mounds and Associated Acrisols in the Coastal Savanna Zone of Ghana and Impact on Hydraulic Conductivity,» Natural Science, vol. 4, no. 7, pp. 423–437, 2012. doi: 10.4236/ns.2012.47058.

[20] S. Zingore, R. J. Delve, J. Nyamangara and K. E. Giller, «Multiple Benefits of Manure: The Key to Maintenance of Soil Fertility and Restoration of Depleted Sandy Soils on African Smallholder Farms,» *Nutrient Cycling in Agroecosystems,* vol. 80, pp. 267–282, 2008. https://doi.org/10.1007/s10705-007-9142-2.

[21] D. Bitom, B. Volkoff, A. Beauvais, F. Seyler and P.-D. Ndjigui, «Rôle des héritages latéritiques et du niveau des nappes dans l'évolution des modelés et des sols en zone intertropicale forestière humide,» *Comptes Rendus Geoscience,* vol. 336, pp. 1161–1170, 2004.

[22] C. Ansart, «Formation des latérites du bouclier amazonien: apports du couplage minéralogie - géochimie - géochronologie,» Ph.D. dissertation, Université Paris-Saclay, Paris, France, 2022. [Online]. Available: https://tel.archives-ouvertes.fr/tel-03646949.

[23] P. Kersting, «Recherches pédo-écologiques dans le Parc National de la Comoé (Côte-d'Ivoire),» *Les Cahiers d'Outre-Mer,* vol. 58, no. 229, pp. 57–80, 2005. https://doi.org/10.4000/com.264

[24] P. Toscano, M. Brambilla, M. Cutini, and C. Bisaglia, «The stony soils reclamation systems in agricultural lands: a review,» *Agricultural Sciences,* vol. 13, no. 4, pp. 500–519, 2022. https://doi.org/10.4236/as.2022.134034.

[25] Soil Survey Staff, *Soil Taxonomy: A Basic System of Soil Classification for Making and Interpreting Soil Surveys,* 2nd ed., Agriculture Handbook No. 436. Washington, D.C.: USDA-NRCS, 1999. [Online]. Available: https://www.nrcs.usda.gov/Internet/FSE_DOCUMENTS/nrcs142p2_051232.pdf